

# Ordovician (Early Darriwilian) Conodonts and Sponges from West of Parkes, Central New South Wales

YONG YI ZHEN<sup>1</sup> AND JOHN PICKETT<sup>2</sup>

1. Palaeontology Section, The Australian Museum, 6 College Street, Sydney, NSW 2010, Australia (yongyi.zhen@austmus.gov.au);
2. Geological Survey of New South Wales, NSW Department of Primary Industries, State Geoscience Centre, 947-953 Londonderry Road, Londonderry, NSW 2753; Research Associate, Australian Museum, Sydney.

Zhen, Y.Y. and Pickett, J.W. (2008). Ordovician (Early Darriwilian) conodonts and sponges from west of Parkes, central New South Wales. *Proceedings of the Linnean Society of New South Wales* 129, 57-82.

A well preserved conodont fauna and an associated small sponge assemblage recovered from a limestone lens exposed on Kirkup Station, 15 km west of Parkes, New South Wales are described and illustrated. The conodont fauna is exceptionally rich by Australian standards, represented by nearly 4,000 specimens, but low in diversity including only six species: *Erraticodon balticus* Dzik, 1978, *Kirkupodus tricostratus* gen. et sp. nov., *Protopanderodus* cf. *varicostatus* (Sweet and Bergström, 1962), *Protopanderodus*? *nogamii* (Lee, 1975), *Juanognathus serpaglii* Stouge, 1984, and *Pseudooneotodus mitratus* (Moskalenko, 1973). The species definition of *E. balticus* is revised based on the current collection of over 1,700 specimens. Co-occurrence of *E. balticus*, *J. serpaglii* and *P. cf. varicostatus* suggests an early Darriwilian (Da2) age for the fauna, which is correlated with that from the basal Weemalla Formation exposed further east near Orange. Two anthaspidellid sponges occur in the assemblage. The stromatoporoid *Ianilamina kirkupensis* gen. et sp. nov. is the oldest stromatoporoid reported from Australia, and among the oldest known. A shallow-water, near-shore setting for the fauna is supported by the abundant occurrence of algal oncolites and certain sedimentary features in the limestone lens.

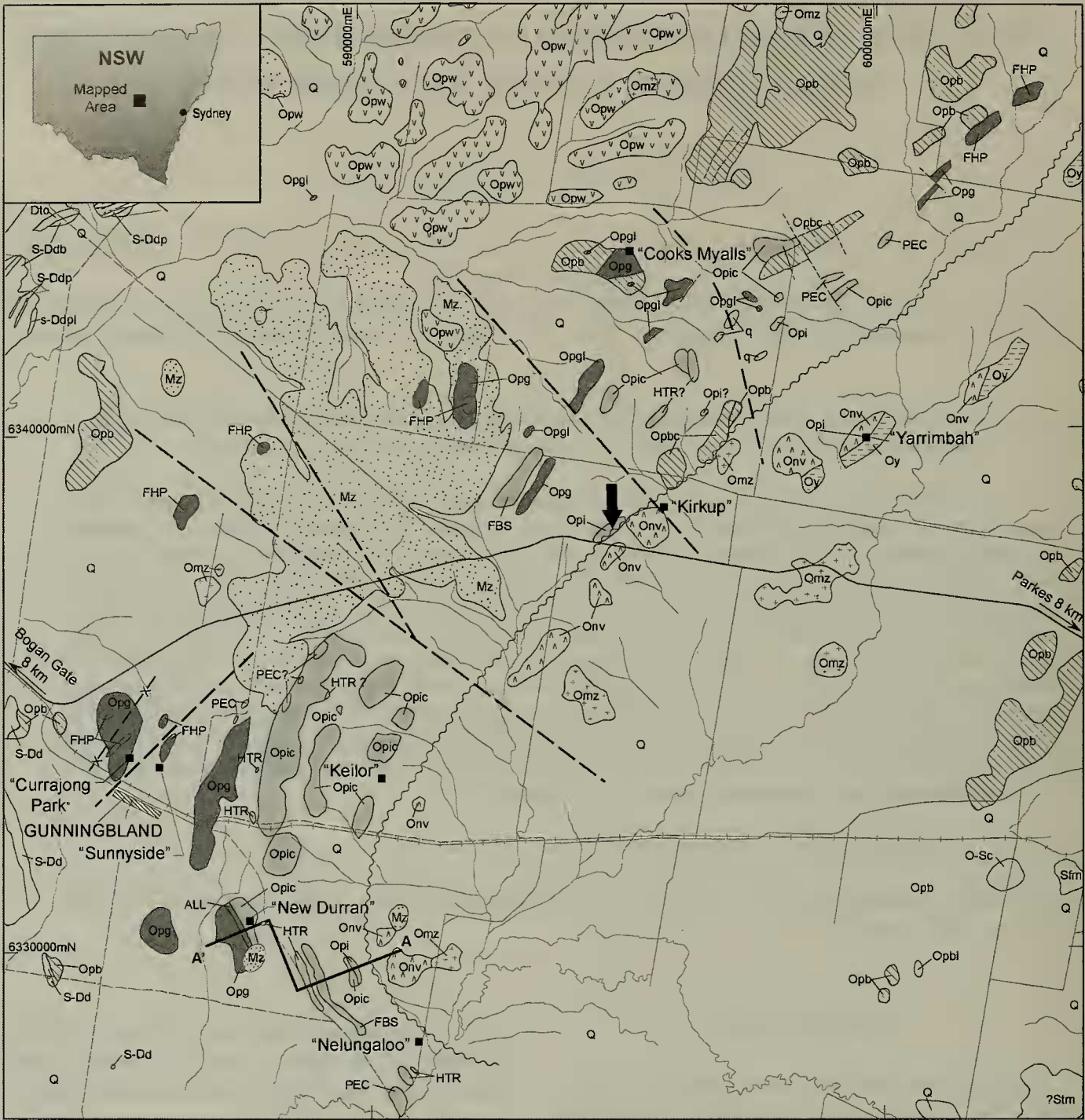
Manuscript received 30 June 2007, accepted for publication 6 February 2008.

**KEYWORDS.** a stromatoporoid, Conodonts, Darriwilian, Goonumbla Volcanics, Middle Ordovician, New South Wales, new taxa, sponges.

## INTRODUCTION

The western flank of the Forbes Anticline, west of Parkes, New South Wales, is made up of a generally conformable succession of andesitic volcanics and diverse, mostly shallow-water sediments of Middle and Late Ordovician age (Fig. 1). An analysis of Late Ordovician coral and conodont faunas in this area was provided by Pickett and Percival (2001). Their assemblages were derived from a series of limestones, mostly not continuous along strike for any great distance, occurring in a series of formations called by them the Goonumbla Volcanics (oldest), the Billabong Creek Limestone and the Gunningbland Formation (youngest). In that paper, the oldest conodont assemblages reported were from a level about 270 m below the top of the Goonumbla Volcanics. The small faunas were not finely age-diagnostic, the only identifiable species being *Periodon aculeatus* Hadding, *Panderodus* cf. *gracilis* (Branson and Mehl)

and *Drepanodus arcuatus* Pander (sample C874, Fig. 2). Some 100 m higher a cluster of samples yielded *Pygodus anserinus* Lamont and Lindström, *Pygodus anitae* Bergström and *Eoplacognathus* spp. A sample from the base of the Billabong Creek Limestone (C828) yielded both *Pygodus anserinus* and *P. serra* (Hadding), indicating that the base of that formation lies within the *kielcensis* Subzone, placing the base of the Billabong Creek Limestone just below the top of the Darriwilian (Da4). Re-examination of the specimen from C828 referred to *P. serra* (Pickett and Percival 2001, fig. 4C) suggests that it is better placed in *P. protoanserinus* Zhang, 1998b, since the distance between the inner and central denticle rows is greater than that between the outer and inner rows. Zhang's fig. 2 suggests that the ranges of *P. anserinus* and *P. protoanserinus* do not overlap, so their co-occurrence implies an age right on the boundary between the *serra* and *anserinus* Zones, and the age can be refined to Da4b. Her detailed analysis



GEOLOGY OF THE GUNNINGBLAND AREA  
West of Parkes, Central New South Wales

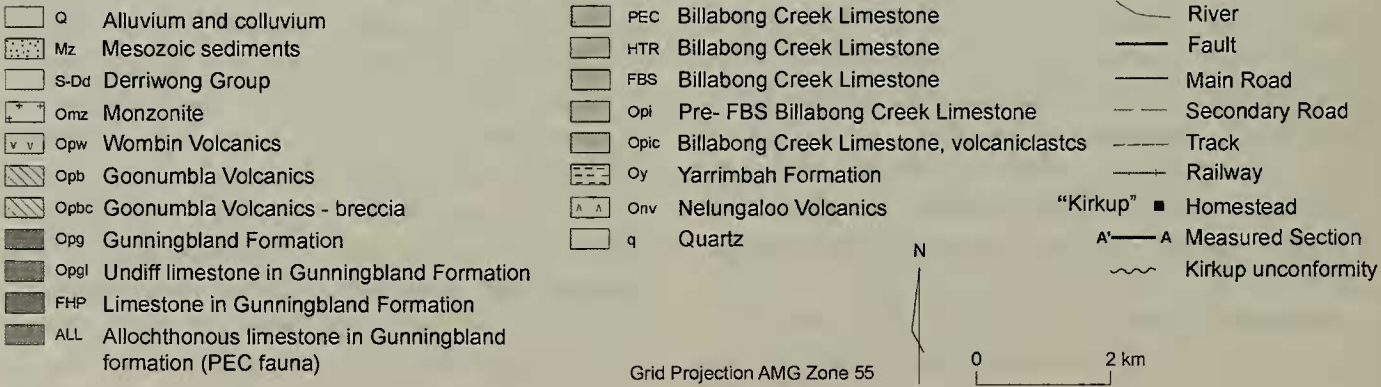


Figure 1. Map of the study area west of Parkes, showing Kirkup locality (arrowed) and location of section A – A'. After Pickett and Percival (2001).



of *Pygodus* species (Zhang 1998b) also indicates no overlap between the ranges of *P. anitae* and *P. anserinus*. The specimen from sample C900 referred to *P. cf. anserinus* (Pickett and Percival 2001, fig. 4G) is a tertiopedate element, and, although more strongly denticulate than that figured by Zhang (1998b, pl. 2, fig. 17), it is possible that it belongs to *P. anitae*, thus removing the anomalous co-occurrence of *P. anitae* and *P. anserinus*. Nonetheless, the presence of *P. anitae*, possibly a later form of the species, since the morphology of the specimen figured by Pickett and Percival (2001, fig. 4D) lies between the two forms figured by Zhang (1998b, fig. 2), indicates the presence of strata at least as old as the top of the *E. suecicus* Zone or basal *P. serra* Zone (upper Da3).

The type locality of the Nelungaloo Volcanics lies in an excavation not more than 100 m stratigraphically below the level of the oldest conodont assemblages in the Nelungaloo section (Fig.1, A-A'). Glen et al. (2007, fig. 3) have indicated the probable presence of Yarrimbah Formation strata between the Goonumbla Volcanics and Nelungaloo Volcanics in this section, as Simpson et al. (2005) have done for the Kirkup area. However, it has not proved possible, at least at Nelungaloo, to date the oldest strata of the Goonumbla Volcanics, and, consequently, the onset of post-unconformity sedimentation, as other than Da3. The interest of the present locality is that it lies but a short interval (a few metres) above the Kirkup Unconformity, and gives the opportunity to constrain the age of the base of the Goonumbla Volcanics (= top of the Kirkup Unconformity, see below) more precisely.

Recently, Simpson et al. (2005) have mapped a widespread unconformity (here named the Kirkup Unconformity) between the Yarrimbah Formation and Goonumbla Volcanics, with the Nelungaloo Volcanics occupying the core of the Forbes Anticline. Their figures 1 and 2 incorporate age determinations purportedly derived from information in Pickett and Percival (2001). There appear, however, to have been some errors in transcribing the data to their figures, since the localities bearing the ages Da2 and Da4, and lying north and slightly west of "Nelungaloo" homestead, are those referred to above as Da3 and Da4, respectively. Additionally, the locality with age Da4, just southwest of "Kirkup" homestead, is that of the locality forming the focus of the present report, and for which no age has been given either by Pickett and Percival (2001) or any other authors to date. No assemblages as old as Da2 were reported by Pickett and Percival. Consequently, the data shown by Simpson et al (2005) as indicating the age of the youngest post-unconformity strata are misleading.

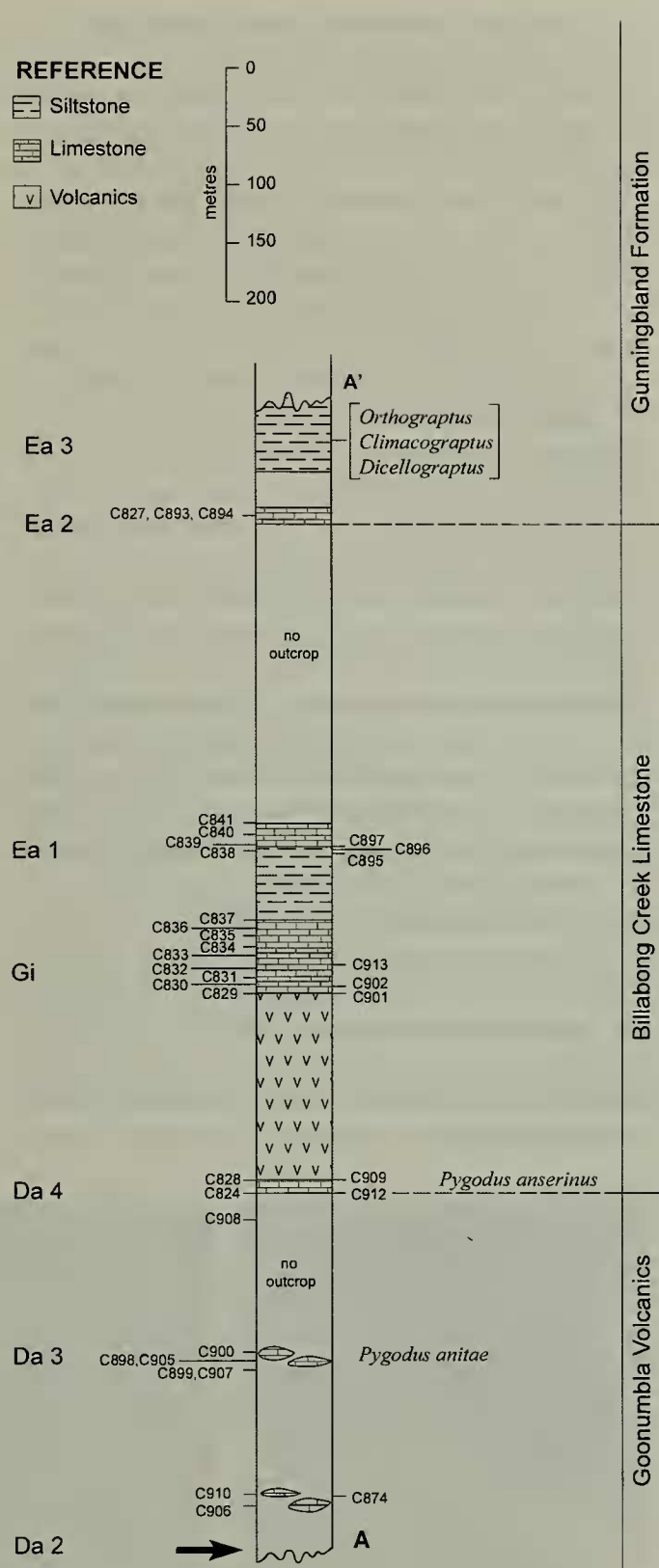


Figure 2. Stratigraphic section A – A' from Fig. 1, showing location of samples discussed in the text, the level of the sampled limestone lens at Kirkup correlated back to this section (arrowed), and ages in terms of the Australian Ordovician stages (Da = Darriwilian, Gi = Gisbornian, Ea = Eastonian).

# BIOSTRATIGRAPHY AND BIOFACIES

The association of *Juanognathus serpaglii*, although very rare, with abundant *Erraticodon balticus* and *Protopanderodus* cf. *varicostatus* in the Kirkup fauna indicates an early Darriwilian age (Da2, upper *variabilis* Zone) for the fauna. This age determination is also supported by the occurrence of *E. balticus* in the basal Weemalla Formation exposed in the Panuara district, southwest of Orange in central New South Wales. In the basal Weemalla Formation, *E. balticus* (referred to as *E. sp.*) was found co-occurring with *Ansella jemtlandica*?, *Periodon macrodentatus*, *Drepanodus?* *bellburnensis*, *Paroistodus originalis*?, *Protopanderodus cooperi*, *P. robustus*, *P. varicostatus*, and *Dzikodus humanensis*, which also suggested an early Darriwilian (Da2) age (Zhen and Percival 2004b). This age for the base of the Weemalla Formation is consistent with the Da3 graptolite occurrence at a higher level in the unit (Smith 1966; Zhen and Percival 2004b). In the Table Head Formation of western Newfoundland, *Juanognathus serpaglii* and *Erraticodon balticus* occur together in the upper part of the *Histiodelpha tableheadensis* Assemblage Zone, which was correlated with the upper *variabilis* Zone (Stouge 1984).

In his study of the conodont faunas from the Table Head Formation Stouge (1984) recognized a *Parapanderodus-Scalpellodus* biofaces, which was further subdivided into an inner shelf sub-facies dominated by the occurrence of *Erraticodon balticus*, and an outer shelf sub-facies characterized by the

dominant occurrence of *Ansella*. The Kirkup fauna with its dominance of *E. balticus* and *Kirkupodus tricostatus* gen. et sp. nov. is most similar to the fauna of the inner shelf sub-facies of the *Parapanderodus-Scalpellodus* biofacies.

# SAMPLING LOCALITIES

The limestone yielding the assemblage reported here lies on Kirkup station, 15 km west of the town of Parkes in the central west of New South Wales (Fig. 1). The outcrop extends for a few hundred metres, from approximately GR 594700 6237900 to GR 595000 6238300 (m, AMG; Parkes 1:50,000 sheet, 8531 I & IV). Its thickness is about 1.5 m, though the tumbled nature of the outcrop hinders accurate measurement.

In addition to the extensive conodont assemblage which affords the basis of the age determination, there is a small fauna of anthaspidellid sponges, all of which are completely desilicified and broken, and the stromatolite-like stromatoporoid *Ianilamina* which is quite common and reaches considerable size. A few, generally damaged brachiopods and rare gastropods are the only other macrofossils. The macrofossils occur in the more terrigenous parts of the unit. Algal oncolites with abundant *Girvanella* are not uncommon (Fig. 3A, B), oolites occur frequently although a true oolitic limestone is never developed, and there are patches of a coquina of small shells most of which lie in the concave-up position (Fig.

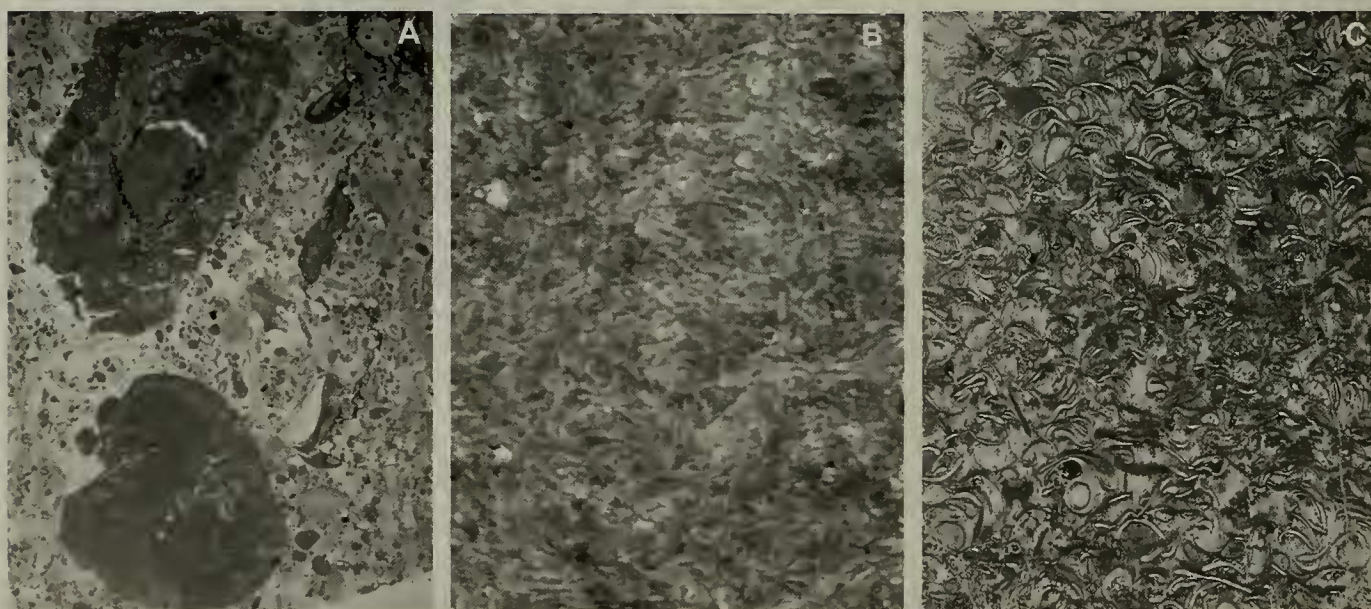


**Figure 3.** Sedimentary features of the limestone lens at Kirkup. A, thin section of oncolites, MMF 44877, x 3.7. B, detail of the smaller oncolite, showing tubes of the alga *Girvanella* sp., x 40. C, vertical thin section of coquina of small shells, younging upward, MMF 44874, x 4.6.



	C1849	C2297	C2298	C2299	C2300	C2301	C2302	C2339	C2340	C2341	C2342	C2343	C2344	C2345	C2346	C2347	Total
		5	1	17	17	50	1	33	295	224	242	181	86	105	348	109	1726
	<i>Erraticodon balticus</i>				1	3		1	28	20	69	47	26	4	78	16	295
	<i>Protopanderodus</i> cf. <i>varicostatus</i>					2		3	84	59	66	69	41	12	98	21	458
	<i>Protopanderodus</i> ? <i>nogamii</i>					16		4	194	102	294	223	99	78	346	102	1480
	<i>Kirkupodus tricostratus</i> gen. et sp. nov.	3			5												3
	<i>Juanognathus serpaglii</i>										1	2				1	1
	<i>Pseudooneotodus mitratus</i>																
	Total	26	8	1	22	23	71	41	601	405	672	522	252	199	870	249	3963

Table 1. Distribution of conodont species in samples from the limestone lens exposed near Kirkup Station, Gunningbland, New South Wales (samples C2340 - 2347 collected from calcarenite).

3C). Sedimentary features are thus in accord with a shallow-water situation, well within the photic zone and above wave-base, and tally with its position immediately above the Kirkup Unconformity.

There are two major lithologies in the limestones recognized in the outcrop, calcarenite and packstone. Conodonts were rare in the former, but very abundant in the greyish fine grained packstone (see Table 1).

SYSTEMATIC PALAEONTOLOGY

Illustrations in Figures 3-4 are optical microscopic photographs of thin sections in transmitted light. These specimens bear the prefix MMF, and are housed at the Londonderry Geoscience Centre of the Geological Survey of New South Wales. Many of the sections used in this study were made well prior to identification of the taxa, and some of the originally numbered specimens contain more than one species. Consequently, parts of and thin sections from a single block are differentiated by a lower case letter appended to the specimen number. All photographic illustrations shown in Figures 5 to 11 are SEM photomicrographs of conodonts captured digitally (numbers with the prefix IY are the file names of the digital images) and are held in the Palaeontology Section of the Australian Museum. Figured specimens bear the prefix AM F. and are deposited in the type collections of the Palaeontology Section at the Australian Museum in Sydney. Conodont samples with the prefix C form part of the collections of the New South Wales Geological Survey at Londonderry.

Phylum PORIFERA Grant, 1836  
Class DEMOSPONGIAE Sollas, 1885  
Informal taxon LITHISTIDA Schmidt, 1870  
Family ANTHASPIDELLIDAE Ulrich, 1889  
Genus *Patellispongia* Bassler, 1927

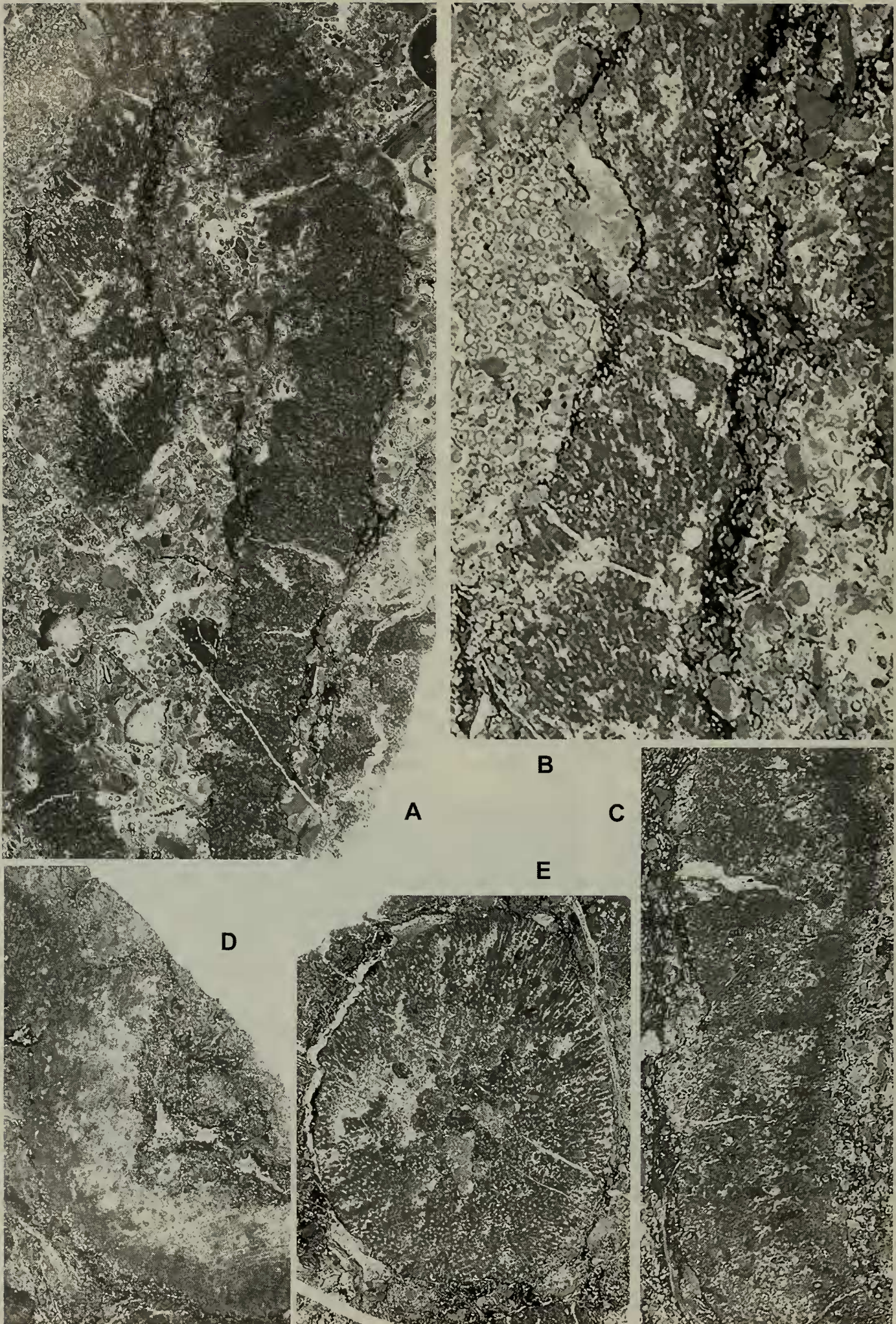
Type species  
*Patellispongia oculata* Bassler, 1927

?*Patellispongia* sp.  
Figures 4A – 4E

Material  
Several large fragmentary sponges (MMF29060, 29069, 29978, 29979, 35561b, 44871-3), with five thin sections.

Description  
In hand specimen the material presents the







appearance of a bladed or occasionally possibly patellate sponge. The thickness of the soma varies from 4.5 to 9.5 mm, with a lateral dimension which may exceed 12 cm. The fragments are all firmly embedded in matrix, so that the precise shape of the sponge cannot be determined, as is the case for its surface, though this appears to be undulose and somewhat uneven.

The thin sections are more or less random, but those that have an orientation nearly parallel to the growth direction show an axis of divergence of the trabs which is much closer to one side of the soma than the other, interpreted as the inner, or, possibly, the excurrent surface. The trabs are 0.2 – 0.25 mm wide and separated by a distance of 0.3 – 0.5 mm. The shafts of the dendroclones are c. 0.07 mm in diameter, and clearly show the typical ladder-like anthaspidellid arrangement. No details of coring or accessory spicules could be observed due to calcification.

### Remarks

Although the specimens are all fragmentary, the manner in which the trabs diverge is similar to that of *Patellispongia australis* Rigby and Webby, as figured by them (1988, pl. 13, fig. 3). In that species the axis of divergence of the trabs lies much nearer to the upper, or concave surface, and this is the basis for the interpretation of the present material. *P. australis* has coring monaxons and, to judge by pl. 13, fig. 9 of Rigby and Webby (1988), also oxeas which lie free in the spicule network. Calcification precludes obtaining any further confirming evidence from our material.

### Anthaspidellid gen et sp. unident.

Figure 4F

### Material

A single specimen with one good transverse section, MMF44878, a probable second specimen, MMF35561a, and a third specimen too small for sectioning, MMF29070.

### Description

Body of sponge cylindrical or possibly obconical, reaching 2.5 cm in diameter, and probably exceeding this in length. The axial area is occupied by a bundle of rounded excurrent canals 1.3 – 2.0 mm in diameter,

the group itself about 1 cm across, and comprising roughly 20 canals, separated by a screen made of up of a single layer of spicules. Details of the exterior are unknown, but it is apparently fairly smooth. The offcut from the transverse section suggests that the excurrent canals end in an apical depression, but if so it was probably shallow. There is no indication of a dermal layer of differentiated spicules, but the sponges were probably somewhat eroded.

The skeleton is typically anthaspidellid, the trabs made up of fused spicule rays and reaching a maximum diameter of 0.3 mm. The trabs are near vertical at the axis, but diverge and are nearly horizontal at the periphery. Between the trabs the spicule shafts are 0.25 – 0.3 mm apart. The material is entirely desilicified, and it is not possible to determine if the trabs include coring spicules.

### Affinities

The scant material and its preservation make a generic assignment hazardous. Of the more or less cylindrical anthaspidellids described by Rigby and Webby (1988) only those ascribed to *Aulocopium* and *Hudsonospongia* can be compared with the present specimen, although it appears to lack the deep apical spongocoel of those forms. The former genus has since been transferred to the family Streptosolenidae (Finks et al. 2004), but in the present material the dendroclones lie parallel to the surface, as is characteristic of Anthaspidellidae.

Class STROMATOPOROIDEA Nicholson and Murie, 1878

Order ?CLATHRODICTYIDA Bogoyavlenskaya, 1969

Family unassigned

*Ianilamina* Pickett and Zhen gen. nov.

### Type species

*Ianilamina kirkupensis* Pickett and Zhen sp. nov.

### Remarks

The genus is named for our friend and colleague Dr Ian Percival, in recognition of his contribution to knowledge of the Ordovician System in New South Wales.

**Figure 4 (LEFT).** Anthaspidellid sponges from Kirkup. A – E, ?*Patellispongia* sp. A, longitudinal (left) and near transverse (right) sections of two specimens, MMF 44872, x 2.8. B, detail of left specimen from A, showing locus of axis of divergence of trabs close to right side of skeleton, x 7.1. C, section of blade, MMF 35561b, x 4.2. D, section of curved blade, MMF 29060a, x 1.7. F, anthaspidellid gen. et sp. unident., MMF 44878, x 2.4.

### Diagnosis

A stromatoporoid whose skeleton consists of thin, extensive, densely porose laminae, with a thread-like tissue occupying some latilaminae.

### *Ianilamina kirkupensis* Pickett and Zhen sp. nov.

Figure 5

### Material

MMF29887 (holotype), paratypes MMF35560, MMF44870, 44875, 44876, 44879; eight thin sections.

### Description

The organism forms stromatolite-like bodies, initially broadly encrusting, but rapidly developing a domical shape, sometimes expanding upwards. The margins are smooth rather than ragged, the major bursts of growth in macroscopic appearance being more or less enveloping. These bodies reach dimensions greater than 12.5 cm wide and 9 cm high. The largest specimen (MMF44879) is an irregularly laminate body with undulose laminae and many inclusions of sediment, and spreading to a width of at least 20 cm, while not more than 7 cm high; the holotype is domical, 20 cm x 14 cm and 11 cm high. The skeleton is comprised of latilaminae (= incremental units of Stearn and Pickett, 1994) which range from 0.1 mm to 1.3 mm in thickness, are discontinuous laterally, and present varying appearance in longitudinal section, due in the main to diagenetic features. The upper surfaces of the latilaminae are defined by the thin laminae, which are remarkably smooth, appear as a very thin, discontinuous, dark line, which, in areas where there has been development of sparry calcite, usually simply vanish, though this can be seen to be a progressive degradation of the structure during diagenesis. The laminae frequently are turned down to terminate on the upper surface of the previous lamina (Fig. 5E).

Some latilaminae present a brown and rather flocculent appearance between the laminae. Others

are light in colour, demarcated by the dark line (lamina) on their upper surface, and show internally a vague network of thread-like calcified tissue, whose structure is not clearly delineated and is never as strongly calcified as the laminae (Fig. 5F). The appearance of these layers intergrades with that of the brownish, flocculent layers, so it is probable that the latter are layers which have undergone more diagenetic alteration.

In tangential section the thin, dark laminae can be seen to be minutely, irregularly porous (Figs 5F, 5J). The pores are subangular to subrounded, have an internal diameter of 0.05 – 0.1 mm, and are separated by a delicate meshwork of calcified tissue about 0.025 mm wide between the pores. No structures approximating to astrorhizae have been identified.

### Associated features

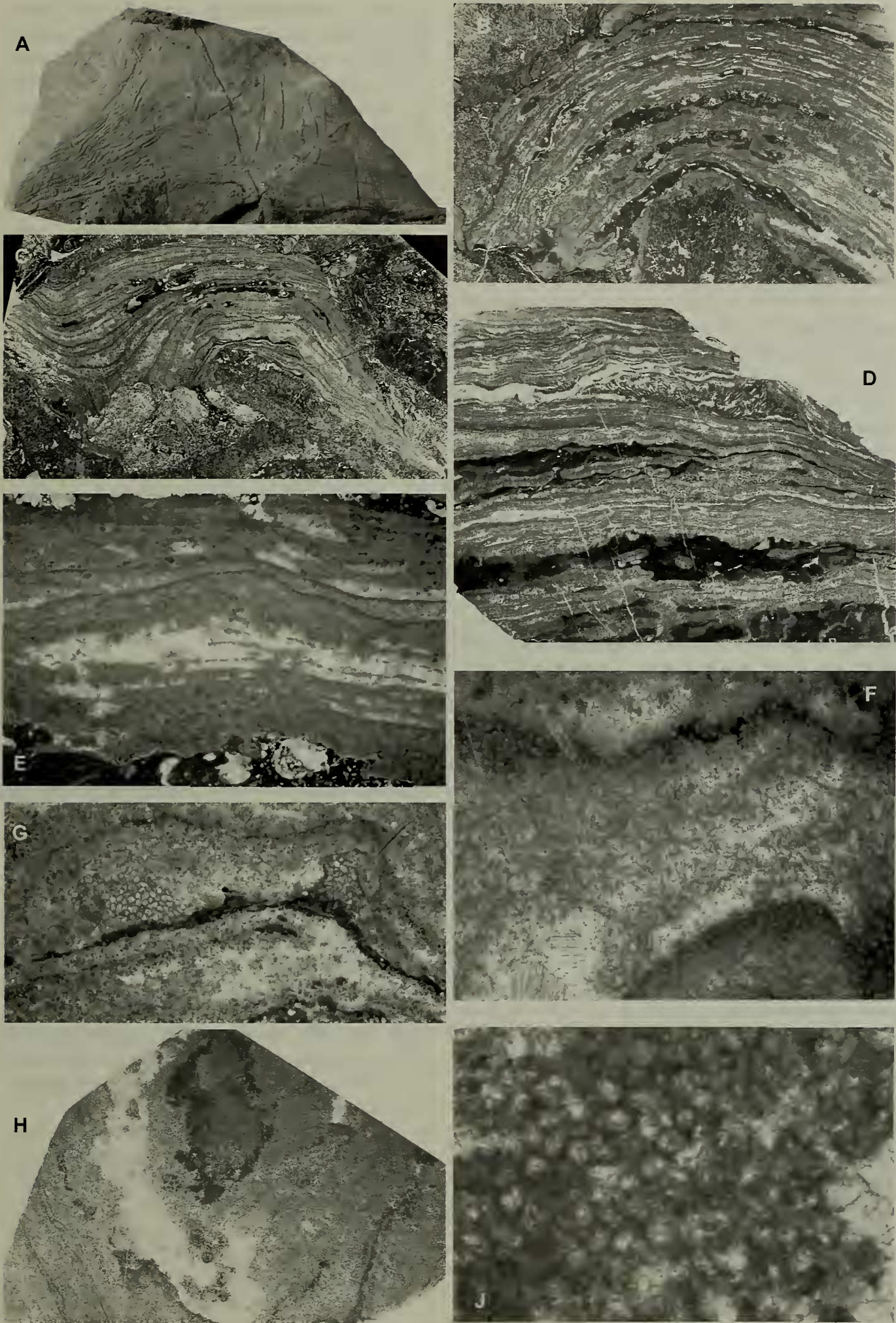
The vertical succession of latilaminae is occasionally interrupted. This is most commonly the result of accumulation of sediment on the surface, which is then covered by the next incremental unit (Fig. 5B). Interruptions may also be caused by algal mats in which tubes of *Girvanella* may clearly be seen, or by overgrowth by an unidentified anthaspidellid sponge (Fig. 5D). Finally, there are small encrustations of what are probably the early stages of bryozoan colonies (Fig. 5G) or possibly algae, but the small size of these (c. 1 mm, with tubes 0.075 – 0.1 mm in diameter) suggests that they were rapidly overgrown by the stromatoporoid.

### Remarks

The most similar form described so far is the marginally older *Zondarella* Keller and Flügel, 1996, from the late Arenig (= earliest Darriwillian of Argentina). The type species, *Z. communis*, forms large, stromatolite-like masses which even construct reefs, quite different from the scale of the present occurrence. The poorly developed vertical elements of *Ianilamina* resemble to some extent those of *Zondarella*, but the well developed pores in the laminae of the former have not been described from

**Figure 5 (RIGHT).** *Ianilamina kirkupensis* gen. et sp. nov., all from a limestone lens at the base of the Goonumbla Volcanics, Kirkup station, Gunningbland, NSW. A, appearance in hand specimen, MMF 44870b, x 0.6. B – F, longitudinal sections. B, MMF 44876, encrusting on anthaspidellid sponge (lower centre), x 1.2. C, MMF 44875a, also encrusting an anthaspidellid, x 1.2. D, section MMF 35560a, specimen with rather flat laminae, and enclosing a small anthaspidellid (top right), x 1.4. E, detail of B, showing terminations of laminae, x 6.8. F, somewhat oblique section through one incremental unit, showing porous laminae and thread-like internal structure, MMF 44875b, x 13.2. G, detail of C, showing small encrusting ?bryozoans, overgrown by later incremental units, x 10.5. H, tangential section of holotype MMF 29887b, section has traversed a rather flat lamina (dark area, top centre), x 1.7. J, detail of central part of H, showing detail of the pores in the lamina, x 49.







*Zondarella*. On the other hand, breaks in the laminae of *Zondarella* are quite common (e.g. Keller and Flügel 1996, pl. 47, fig.6), and it may be that these equate to the pores of *Ianilamina*. The epizoid ?bryozoans illustrated by Keller and Flügel (pl. 47, fig. 8) are almost identical with those observed on *Ianilamina*. Photographs of thin sections of topotype specimens of *Zondarella communis*, kindly supplied by Dr Marcelo Carrera, do not show laminae with pores similar to those of *Ianilamina*. *Zondarella* was assigned to the family Pulchrellaminidae Webby 1993, which was included questionably as the last family in the order Labechiida by Webby, in Stearn et al. (1999). The soft tissue of members of that order appears to have been external to the skeleton, whereas the anatomy of most other stromatoporoid groups suggests, by analogy with *Vaceletia*, e.g. Stearn and Pickett (1994), that most of the soft tissue was internal. In spite of other similarities with *Zondarella* the absence of pores in that genus is particularly significant, pointing to labechiid affinities. The pores of *Ianilamina* however imply relationship to non-labechiid stromatoporoids, and for this reason the genus is tentatively included amongst the clathrodictyids.

A corollary of the virtual absence of pillars or other well calcified vertical structures between the laminae would have been a skeleton which was relatively weak structurally. In spite of this, there is very little evidence of internal damage, although a number of the specimens have clearly suffered external damage.

There has been much discussion with colleagues over the affinities of this material. The preliminary field identifications cast it as stromatolitic, chiefly perhaps due to the rather straggly outline of the individual masses; and indeed, many layers within them are clearly sedimentary. It is possible that the structures here interpreted as porous laminae may be residual features of algal structures otherwise destroyed by diagenetic processes. However, the following features have swayed the interpretation as a stromatoporoid: 1) in addition to the layers of sediment, sponges and bryozoans mentioned above, there are occasional layers of undoubted algal mats, clearly differing in preservation and structure from the tissue immediately surrounding them; 2) the porous laminae are extremely thin, while the true algal layers have a substantial vertical dimension; 3) the laminae turn down rather abruptly to terminate cleanly on the surface of the lamina beneath, suggesting incremental growth rather than surficial accumulation of sediment. The problems faced in the interpretation of *Ianilamina* are in effect the same as those experienced by Keller and Flügel (1996) when describing *Zondarella*, and

efficiently summarised by them (p. 186). Many of their comments also are relevant to the present material, noting particularly the association with a high-energy environment, provision of a hard surface for encrusting organisms, and layers of different composition or structure.

Phylum CHORDATA Balfour, 1880

Class CONODONTA Pander, 1856

Order PRIONIODINIDA Sweet, 1988

Family CHIROGNATHIDAE Branson and Mehl,  
1944

**Genus *Erraticodon* Dzik, 1978**

## Type species

*Erraticodon balticus* Dzik, 1978.

## Diagnosis

Septimembrate or octomembrate apparatus with a ramiform-ramiform structure including makellate M, alate Sa, bipennate Sb and Sc, tertiopectate or tripennate Sd, digyrate Pa, trigyrate Pb, and often tripennate Pc, hyaline elements with a prominent cusp, discrete peg-like denticles on the processes, and a shallow basal cavity.

## Discussion

Represented by at least 10 species with high morphological variation, *Erraticodon* consisting of large, hyaline ramiform elements is an easily recognizable common element in shallow-water, inner-shelf conodont faunas. A number of *Erraticodon* species with a septimembrate or octomembrate apparatus have been recently documented from late Early and Middle Ordovician strata in Australia (Zhen *et al.* 2003, Zhen and Percival 2004a, Zhen and Percival 2004b, Zhen and Percival 2006; Nicoll and Kelman 2004) and in South China (Zhen *et al.* 2007). Known as the oldest genus in the family Chirognathidae (Sweet 1988), *Erraticodon* was geographically widely distributed with a stratigraphic range from the late Early Ordovician (*evae* Zone) to the late Mid Ordovician (Darriwilian) (Zhen *et al.* 2007). The following species are assigned to *Erraticodon*:

*Erraticodon balticus* Dzik, 1978; defined herein as having a septimembrate apparatus; type material from an erratic boulder of Middle Ordovician (possibly early Darriwilian) age, found near Kartuzy, Poland. It was also recorded from the lower Darriwilian (Da2) of Newfoundland (Stouge 1984), and central New South Wales (this study).

*Erraticodon bellevuensis* Zhen and Percival



2004a; reported as having a septimembrate apparatus (Zhen and Percival 2004a, p. 94-96, figs. 12, 13), from allochthonous limestone (Middle Ordovician, Darriwilian, ?Da3) in the Oakdale Formation of central New South Wales.

*Erraticodon fenxiangensis* Ni, in Ni and Li 1987; not adequately documented, four morphotypes referable to M, Sa, Sb and Sc elements recognised (see Ni, in Ni and Li 1987, p. 408-409, pl. 60, figs. 6=Sc, 7=Sa, 14=Sb, 15=M), from the lower and middle parts of the Guniutan Formation (Middle Ordovician, Darriwilian) of Yichang, Hubei, South China.

*Erraticodon gratus* (Moskalenko, 1977) (see Moskalenko 1989); recorded as having a septimembrate apparatus, from the Ordovician of Russia.

*Erraticodon hexianensis* An and Ding, 1985; revised as having an octomembrate apparatus (An and Ding 1985; Zhen *et al.* 2007), from the late Dawanian to early Darriwilian of South China.

*Erraticodon patu* Cooper, 1981; recorded as having a septimembrate or possibly octomembrate apparatus (see Zhen *et al.* 2003; Nicoll and Kelman 2004) from the Horn Valley Siltstone (Early Ordovician, *evae* Zone) of the Amadeus Basin of central Australia, and also reported from the Tabita Formation (and various other units of the same age) in western New South Wales (Zhen *et al.* 2003, Zhen and Percival 2006).

*Erraticodon tangshanensis* Yang and Xu, in An *et al.* 1983; reported having a septimembrate apparatus (see An *et al.* 1983, p. 95-97), from the Majiagou Formation and Beianzhuang Formation of Middle Ordovician age in North China.

*Erraticodon tarimensis* Zhao *et al.* 2005; reported as having a septimembrate apparatus (Zhao *et al.* 2005, p. 30, pl. 2, figs 1-13), from the middle part of the Upper Qiulitag Formation (late Early Ordovician) in the Tarim Basin of Northwest China.

*Erraticodon* sp. Löfgren, 1985 (p. 124, fig. 4AT-AY); with M, Sc, Pa, and Pb? (or Sa?) elements illustrated from core samples of Middle Ordovician age (upper *para* to lower *variabilis* zones) at Finngrundet, south Bothnian Bay, Sweden.

### ***Erraticodon balticus* Dzik, 1978**

Figures 6-8

#### **Synonymy**

*Erraticodon balticus* Dzik, 1978, p. 66-67, text-fig. 6a-e, pl. 15, figs 1-3, 5-6 (text-fig. 6d and pl. 15, fig. 5 = M element; text-fig. 6e and pl. 15, fig. 6 = Sa

element; text-fig. 6c and pl. 15, fig. 3 = Sb element; text-fig. 6a and pl. 15, fig. 1 = Sc element; text-fig. 6b and pl. 15, fig. 2 = Sd element); Stouge 1984, p.84-85, pl. 17, figs 9-19 (fig. 11 = M element; figs 17-18 = Sa element; figs 9-10 = Sb element; fig. 19 = Sc element; figs 13-15 = Sd element; figs 12, 16 = Pb element).

*Erraticodon* sp. Zhen and Percival 2004b, p. 167-168, figs 8A-H, 9A-I (9A-B=M element; 9C-G=Sa element; 9H=Sb element; 9I=Sc element; 8A-B and 8H=Pa element; 8C-G=Pb element).

#### **Material**

1726 specimens recovered from 16 samples (see Table 1) collected along the strike of the 1.5 m thick limestone lens.

#### **Diagnosis**

A species of *Erraticodon* with a septimembrate ramiform-ramiform apparatus, including makellate M, alate Sa, bipennate Sb and Sc, tripennate (modified bipennate) Sd, digyrate Pa, and trigyrate (modified digyrate) Pb elements; all elements hyaline with a prominent cusp, and discrete, peg-like denticles on the processes, and a shallow open basal cavity often with basal cone attached; Sa element with short lateral processes each bearing a single denticle and with a long posterior process; Sa, Sb and Sc elements with an excessively enlarged denticle (location varying from the first to fourth away from the cusp) developed on the posterior process.

#### **Description**

M element makellate (Fig. 6A-D) with a long outer lateral process bearing four to seven pointed denticles, and a sharp costa along the inner lateral face with neither denticles nor anti-cusp (Fig. 6A); cusp robust, antero-posteriorly compressed, and distally curved posteriorly, with broad anterior and posterior faces, and sharp costate lateral margins (Fig. 6A-C); basal buttress weakly developed on the posterior face (Fig. 6C); basal cavity shallow, tapering into narrow groove towards the outer lateral end of the base (Fig. 6A-B) with gently arched basal margin in anterior (Fig. 6D) or posterior view (Fig. 6A).

Sa element alate, symmetrical, bearing a long denticulate posterior process, and a short lateral process on each side with a single denticle (Fig. 6E-K); cusp triangular in cross section with a broad anterior face, and a sharp costa along its posterior margin and on each antero-lateral side; three sharp costae extending basally and merging with the upper margin of the posterior and the lateral processes; posterior process long, in most specimens broken



Figure 6. *Erraticodon balticus* Dzik, 1978 A-D, M element; A, AM F.133041, C2340, posterior view (IY85004); B, AM F.133042, C2340, basal view (IY85003); C, AM F.133043, C2340, upper view (IY85005); D, AM F.133044, C2340, anterior view (IY85001). E-K, Sa element; E-G, AM F.133045, C2340, E-F, anterior views (IY85022); G, upper view (IY85023); H, AM F.133046, C2343, lateral view (IY85010); I-J, AM F.133047, C2340, I, posterior view (IY85020), J, basal view (IY85021); K, AM F.133048, C2342, lateral view (IY88017). L-P, Sb element; L, AM F.133049, C2340, inner lateral view (IY85018); M-N, AM F.133050, C2342, M, basal view (IY87033), N, inner lateral view (IY87034); O, AM F.133051, C2340, upper view (IY85019); P, AM F.133052, C2343, outer lateral view (IY85010). Scale bars 100  $\mu$ m.



before or after the excessively larger denticle, which is typically the first or second denticle away from the cusp, and typically over twice as wide as the cusp on lateral view (Fig. 6K); single denticle on lateral processes antero-posteriorly compressed with a broad anterior and posterior face and a sharp edged lateral side; basal cavity shallow and small with strongly arched basal margin in lateral view (Fig. 6H, K).

Sb element bipennate, asymmetrical with a sub-erect cusp, a long posterior process, and a downward extending and strongly inner laterally curved anterior process (Fig. 6L-P); cusp moderately compressed laterally with a sharp anterior costa and a posterior costa that extends downward to form the upper margin of the anterior and posterior processes (Fig. 6O); posterior process long, bearing more than five denticles, with the third or fourth denticle away from the cusp excessively larger than other denticles, typically as large as the cusp (Fig. 6L) or even larger (Fig. 6N-O); denticles on posterior process moderately compressed laterally with a sharp costa along the anterior and posterior margins; long anterior process strongly curved inward forming an angle of about 90° or less with posterior process (Fig. 6M, O), and bearing five to eight or even more denticles, which are more closely spaced than those on the posterior process, and laterally compressed with sharp edges; basal cavity shallow, often with basal cone attached, showing a sickle-like outline in basal view (Fig. 6M).

Sc element bipennate (Fig. 7A-E) with a prominent cusp, a downwardly extended, slightly inner laterally curved anterior process bearing three or more denticles (Fig. 7C), and a long posterior process bearing four or more long denticles (Fig. 7C-D); cusp laterally strongly compressed with sharply costate anterior and posterior margins and smooth lateral faces; one denticle on posterior process (typically the third away from the cusp) excessively larger than other denticles; basal cavity shallow with an arched basal margin in lateral view (Fig. 7D).

Sd element tripennate (modified bipennate) with a prominent cusp, a short anterior process bearing two or three denticles, a long posterior process bearing five or more denticles, and a long, outer lateral process bearing up to seven denticles (Fig. 7F-M); cusp tricostrate bearing sharp anterior, posterior and outer lateral costae, which extend downward to merge with the upper margin of the three processes; cusp rounded in cross section (Fig. 7H) with outer lateral costa more towards posterior, and curved inner laterally and posteriorly with broad, convex inner lateral face and antero-outer lateral face, but with slightly concave postero-outer lateral face (Fig. 7H);

anterior process inner laterally curved and extending downward with a straight basal margin nearly normal to the basal margin of the posterior process, denticles closely spaced with smallest at the distal end and the largest, which is only slightly shorter than the cusp, next to the cusp; posterior process long, but broken in most of the specimens recovered; denticles on both anterior and posterior processes compressed laterally, oval in cross section with a sharp costa along their anterior and posterior margins; outer lateral process long, posteriorly curved varying from a 70° angle with the posterior process (Fig. 7G) to nearly parallel with the posterior process (Fig. 7J), denticles moderately compressed antero-posteriorly, oval in cross section with sharply costate lateral margins, and curved posteriorly.

Pa element digyrate with a less prominent cusp, a long sinuously curved inner lateral process, and a long, anteriorly twisted outer lateral process (Fig. 8A-G); cusp rounded in cross section with a sharp lateral costa on each side, and broad anterior and posterior faces; denticles on both processes also rounded or weakly antero-posteriorly compressed; basal cavity shallow and inverted with a shallow pit underneath the cusp (Fig. 8D).

Pb element trigyrate (modified digyrate) with a lateral process on each side, and an anterior process bearing three or more denticles (Fig. 8H-N); cusp less prominent than that of the M and S elements, with a broad posterior face and with a sharp costa along anterior margin, and on each side; outer lateral process long, bearing seven or more denticles; inner lateral process shorter bearing typically two or three denticles, anterior process outer laterally curved; denticles antero-laterally compressed on the lateral processes and laterally compressed on the anterior process; basal cavity shallow with a pit underneath the cusp (Fig. 8N).

## Discussion

The type material of *Erraticodon balticus* was recovered from an erratic boulder found near Kartuzy, Pomerania, Poland, but believed to be transported from the Baltic region. Dzik (1978) originally defined the species as consisting of a seximembrate apparatus, but only five elements including makellate M, alate Sa, bipennate Sb and Sc, and tripennate (modified bipennate) Sd were represented in the type material. However he suggested an additional spathognathiform element (Dzik 1978, Fig. 2 = digyrate Pb element) represented by a specimen illustrated as "*Chirognathus*" sp. by Viira (1974, pl. 11, fig. 22). Subsequently, Dzik (1991) indicated that the species had a septimembrate composition, but





Figure 7. *Erraticodon balticus* Dzik, 1978. A-E, Sc element; A-B, AM F.133053, C2343, A, basal-posterior view (IY85012), B, basal view (IY85013); C, AM F.133054, C2343, inner lateral view (IY85017); D-E, AM F.133055, C2342, D, outer lateral view (IY87031), E, basal view (IY87032). F-M, Sd element; F, AM F.133056, C2340, outer lateral view (IY85009); G-H, AM F.133057, C2343, G, upper view (IY85015), H, close up of upper view showing cross section of tricostate cusp (IY85016); I, AM F.133058, C2343, outer lateral view (IY92029); J-M, AM F.133059, C2343, J, outer lateral view (IY92026), K, upper view (IY92025), L, posterior view (IY92027), M, inner lateral view (IY92028). Scale bars 100 µm.

unfortunately provided neither description nor further details of the revised apparatus. Based on material from the Table Head Formation (Darriwilian, Da2) of western Newfoundland, Stouge (1984) suggested a septimembrate apparatus for *E. balticus*, its elements being comparable with the M, Sa, Sb, Sc, Sd and Pb

elements defined herein from the Kirkup fauna. No Pa element was reported by Stouge, (1984) and his zygognathiform and sannemanulliform elements are interpreted herein as variants of the Sd element with the outer lateral process curved posteriorly in varying degree.



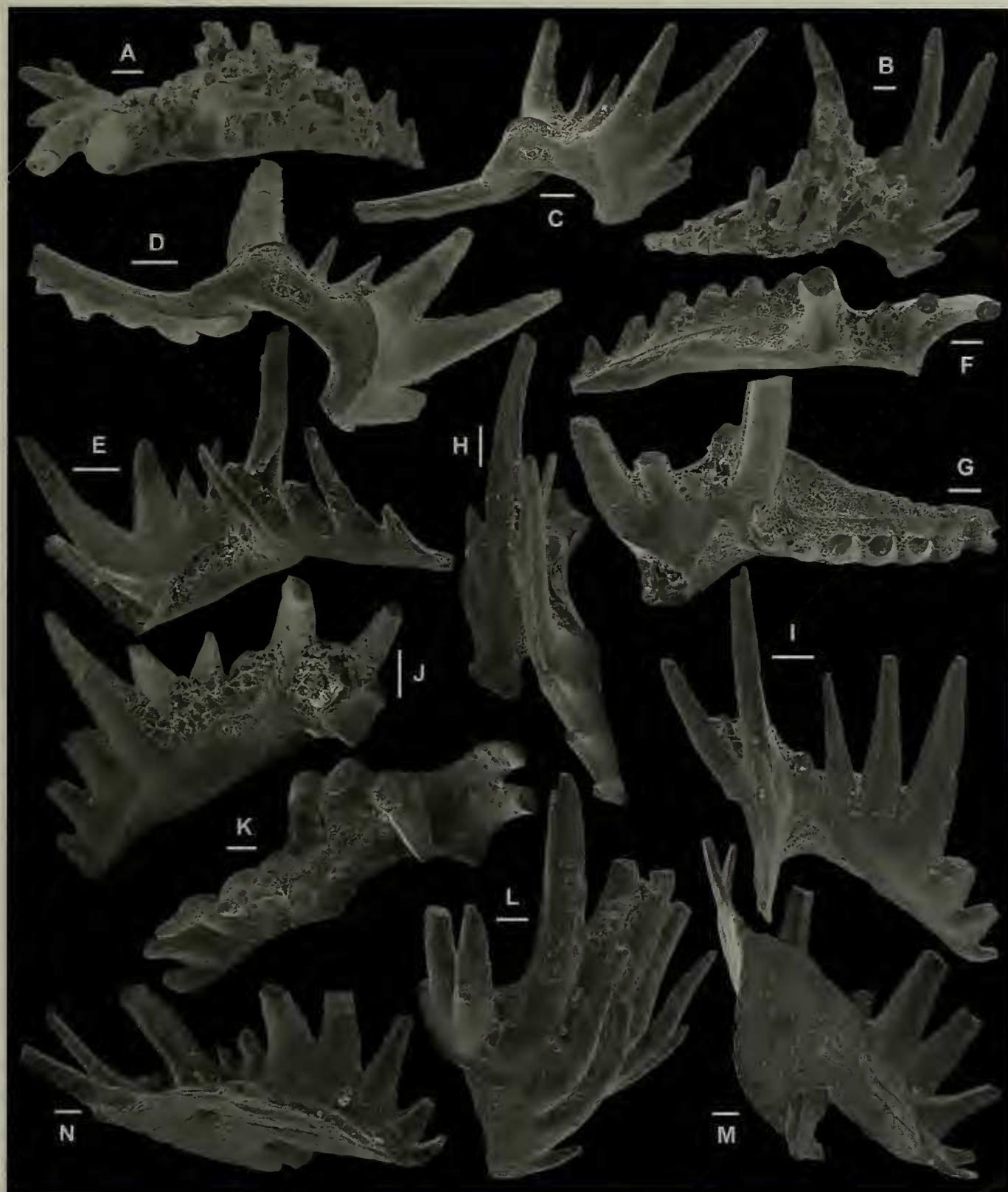


Figure 8. *Erraticodon balticus* Dzík, 1978. A-G, Pa element; A-B, AM F.133060, C2340, A, upper view (IY85008); B, anterior view (IY85006); C-E, AM F.133061, C2342, C, basal-posterior view (IY88011), D, basal view (IY88014), E, anterior view (IY88012); F-G, AM F.133062, C2342, F, upper view (IY88008), G, anterior view (IY88009). H-N, Pb element; H-J, AM F.133063, C2342, H, outer lateral view (IY88003); I, anterior view (IY88002), J, posterior view (IY88004); K-L, AM F.133064, C2300, K, upper view (IY86007), L, inner-anterior view (IY86006); M-N, AM F.133065, C2347, M, basal view (IY88005), N, posterior view (IY88006). Scale bars 100  $\mu$ m.



*E. balticus* is characterized by having an accentuated denticle on the posterior process of the Sa, Sb and Sc elements. The holotype (Dzik 1978, pl. 15, fig. 6) exhibits this accentuated denticle as the third denticle away from the cusp on the posterior process, which is slightly wider (thicker) near the base than the cusp in lateral view. An accentuated denticle similar to that of the holotype was also developed on the posterior process of the Sb and Sc elements in the type material (Dzik 1978, text-fig. 6). In our abundant material from Kirkup, this accentuated denticle on the posterior process of the Sa, Sb and Sc elements is observed as a consistent character, but its position may vary from the first to fourth away from the cusp, and the size can also vary from equal to that of the cusp to over twice its size (Fig. 6K).

Specimens have previously been referred to this species by various authors (e.g. Watson 1988; Lehnert 1995; Albanesi, in Albanesi *et al.* 1998; Zhang 1998a), but their illustrated specimens apparently lack this character and should be excluded from *E. balticus*. For instance, none of the Sa, Sb and Sc elements described by Watson (1988) from the the Goldwyer Formation of the Canning Basin of Western Australia illustrated this diagnostic character of the species. None of the illustrated Sa, Sb and Sc elements referred to as *E. balticus* by either Zhang (1998a, pl. 9, figs 9-10, 13) from the Guniutan Formation in Hubei and

Hunan provinces or by Ding *et al.* (in Wang 1993) from the same stratigraphic unit near Nanjing in South China shows an accentuated denticle on the posterior process. Zhang's (1998a, pl. 9, fig. 9) illustrated Sa element bears more than one denticle on the lateral processes. The material illustrated by Ding *et al.* (in Wang 1993, pl. 37, figs 18-28) as this species includes elements belonging to different genera, and the material illustrated by Zhang (1998a) may be more comparable to *E. hexianensis* (see Zhen *et al.* 2007). That species, recorded from the upper Dawanian to early Darriwilian in South China (Zhen *et al.* 2007), closely resembles *E. balticus*, but its Sa, Sb, and Sc elements lack an excessively enlarged denticle on the posterior process, and its Sd element is tertiopedate rather than tripennate, as in *E. balticus*.

Order PRIONIODONTIDA Dzik, 1976  
Family OISTODONTIDAE Lindström, 1970  
Genus *Juanognathus* Serpagli, 1974

#### Type species

*Juanognathus variabilis* Serpagli, 1974.

*Juanognathus serpaglii* Stouge, 1984

Figure 9C-F



Figure 9. A-B, *Pseudooneotodus mitratus* (Moskalenko, 1973) AM F.133066, C2347, A, upper view (IY92012), B, outer lateral view (IY92013). C-F, *Juanognathus serpaglii* Stouge, 1984. C-D, asymmetrical element, AM F.133067, C2343, C, posterior view (IY92021), D, upper view (IY92022); E-F, symmetrical element, AM F.133068, C2343, E, posterior view (IY92020), F, basal view (IY92019). Scale bars 100 µm.



**Synonymy**

*Juanognathus serpaglii* Stouge, 1984, p. 58-59, pl. 5, figs 10-20 (*cum syn.*).

**Material**

Three specimens, two (both illustrated) from sample C2343, and one from C2342.

**Discussion**

Stouge (1984) originally recognised a bimembrate (symmetrical and asymmetrical) apparatus for the species. Both elements are represented by only one specimen each in our material from Kirkup station. They are identical with the type material from the Table Head Formation of western Newfoundland. Both elements have a cusp with a blade-like costa on each side, broadly convex anterior and posterior faces and a prominent basal surface defined by a ledge-like costa parallel to and slightly above the basal margin, which is similar to that described in *Cooperignathus* Zhen, in Zhen *et al.* 2003 and *Protoprioniodus* Cooper, 1981 (see Zhen *et al.* 2003). This ledge-like costa and basal surface are also well developed in the type material of *J. serpaglii* (Stouge 1984, pl. 5, figs 10, 12, 16), but have not been recognised in the other species of *Juanognathus* including the type species.

Order PROTOPANDERODONTIDA Sweet, 1988  
Family PROTOPANDERODONTIDAE Lindström, 1970

**Genus *Protopanderodus* Lindström, 1971**

**Type species**

*Acontiodus rectus* Lindström, 1955.

***Protopanderodus cf. varicostatus* (Sweet and Bergström, 1962)  
Figure 10A-P**

**Synonymy**

*Protopanderodus cf. varicostatus* (Sweet and Bergström); Löfgren, 1978, p. 191-193, pl. 3, fig. 26-31.

**Material**

295 specimens recovered from 12 samples (see Table 1) collected along the strike of the 1.5 m thick limestone lens.

**Description**

Five morphotypes of this species are recognized and assigned to Sa, Sb, Sc, Pa and Pb elements. Sa element symmetrical, bearing a proclined to suberect

cusp, with a broad anterior face, an antero-lateral costa and a lateral costa on each side, and a costa along its posterior margin (Fig. 10A-E); a broader, shallow groove developed between the two costae and a deep and narrow furrow positioned to the posterior side of the lateral costa. Sb element like Sa, but asymmetrical, with a concave inner face and a convex outer face, and weaker development of the antero-lateral costa on each side, and with a deep furrow developed between the two costae on each lateral face. Sc element strongly asymmetrical and laterally compressed, with a convex outer face bearing a median costa and a furrow to its posterior side, a concave inner face bearing two costae and separated by two furrows (Fig. 10J-K), and with a sharp costa along its anterior and posterior margins. Pa element with a proclined cusp and a shorter base, and with a sharp costa along its anterior and posterior margins; outer lateral face convex and smooth or often with a weak and short postero-lateral costa developed around the curvature of the cusp (Fig. 10M); inner lateral face with two costae and a furrow in between. Pb element like Pa element, but with a suberect cusp and a longer base.

**Discussion**

The current material resembles that described as *Protopanderodus cf. varicostatus* from the Middle Ordovician of northern Sweden (Löfgren 1978), particularly the S elements. The scandodiform Pb elements from the Kirkup fauna generally have a longer base, which was not recognized in *P. varicostatus*, and some of the symmetrical Sa elements show a broader anterior face (Fig. 10A) in comparison with the corresponding elements of *Protopanderodus variabilis*. Some scandodiform P elements of those referred to *Protopanderodus cf. varicostatus* by Löfgren (1978, pl. 3, fig. 30) exhibit intermediate features between the current material, which has a longer base (Pb), and typical *P. variabilis* with a very short base.

***Protopanderodus? nogamii* (Lee, 1975)  
Figure 11A-S**

**Synonymy**

*Scolopodus cf. bassleri* Igo and Koike 1967, p. 23, pl. 3, figs. 7, 8, text-fig. 6B.  
*Scolopodus* sp. A Hill *et al.* 1969, p. O.14, pl. OVII, fig. 13.  
*Scolopodus* sp. C Hill *et al.* 1969, p. O.14, pl. OVII, fig. 15.  
“*Panderodus*” sp. Serpagli 1974, p. 59, pl. 24, figs.





Figure 10. *Protopanderodus* cf. *varicostatus* (Sweet and Bergström, 1962). A-E, Sa element; A-B, AM F.133069, C2343, A, basal-posterior view (IY87005), B, lateral view (IY87004); C-E, AM F.133070, C2342, C-D, lateral views (IY87025, IY87023), E, basal view (IY87026). F-I, Sb element; F-H, AM F.133071, C2343, F, basal view (IY87013), G, inner lateral view (IY87011), H, outer lateral view (IY87014); I, AM F.133072, C2343, inner lateral view (IY87016). J-L, Sc element, AM F.133073, C2343, J, inner lateral view (IY92038), K, upper view (IY92036), L, outer lateral view (IY92037). M-N, Pa element; M, AM F.133074, C2343, outer lateral view (IY87007); N, AM F.133075, C2340, inner lateral view (IY91040). O-P, Pb element; O, AM F.133076, C2340, outer lateral view (IY91038); P, AM F.133077, C2340, inner lateral view (IY91039). Scale bars 100 µm.

12, 13, pl. 30, figs. 12, 13.  
*Scolopodus nogamii* Lee 1975, p. 179, pl. 2, fig. 13.  
*Protopanderodus primitus* Druce (MS), in Cooper 1981 (*nomen nudum*), p. 174, pl. 27, figs. 3, 4 (*cum syn.*); Stait and Druce 1993, p. 307, figs. 13A-C, 18D, E, G-K (*cum syn.*).  
*Scolopodus euspinus* Jiang and Zhang, in An *et al.*

1983, p. 140, pl. 13, fig. 27, pl. 14, figs. 1-8 (*cum syn.*); An and Zheng 1990, p. 173, pl. 2, figs. 7-11, 13, 14, 16.  
*Protopanderodus nogamii* (Lee); Watson 1988: p. 124, pl. 3, figs. 1, 6; Zhen *et al.* 2003, p. 207-209, fig. 23A-P, ?Q (*cum syn.*); Zhen and Percival 2004a, p. 104-105, fig. 18A-K.



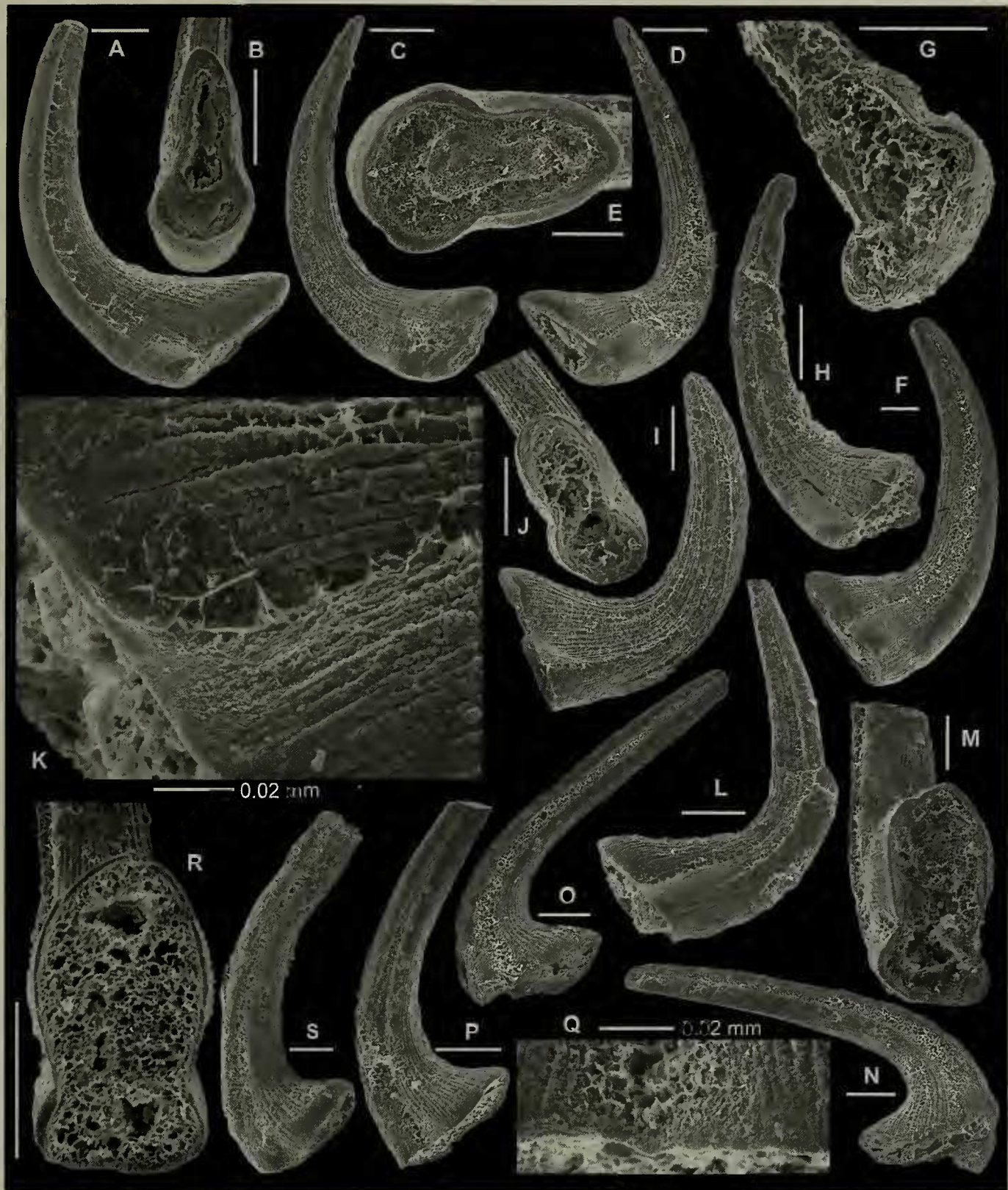


Figure 11. *Protopanderodus? nogamii* (Lee, 1975). A-F, Sa element; A, AM F.133078, C2343, lateral view (IY88032); B-D, AM F.133079, C2343, B, basal view (IY88030), C-D, lateral views (IY88029, IY88031); E-F, AM F.133080, C2340, E, basal view (IY88044), F, lateral view (IY88045). G-H, Sb element, AM F.133081, C2343, G, basal view (IY88035), H, inner lateral view (IY88034). I-L, Sd element; I-J, AM F.133082, C2343, I, inner lateral view (IY88041), J, basal view (IY88039); K-L, AM F.133083, C2343, K, close up showing furrow does not cut through the basal margin and surface striation (IY88038), L, outer lateral view (IY88036). M-O, Pb element; M, AM F.133084, C2343, basal view (IY88018); N-O, AM F.133085, C2343, N, inner lateral view (IY88024), O, outer lateral view (IY88023). P-S, Pa element; P-R, AM F.133086, C2343, P, inner lateral view (IY88027), Q, close up showing furrow does not cut through the basal margin (IY88028), R, basal view (IY88026); S, AM F.1330087, C2343, outer lateral view (IY88021). Scale bars 100 µm, unless otherwise indicated.



*Protopanderodus? nogamii* (Lee); Zhen and Percival 2004b, p. 170-172, fig. 11P, Q.

*Parapanderodus paracornuformis* Ethington and Clark; Albanesi, in Albanesi *et al.* 1998, p. 116, *partim* pl. 12, fig. 13, 8?-10?, *non* 11, 12.

*?Panderodus nogamii* (Lee); Cantrill and Burrett 2004, p. 410, pl. 1, figs 1-16.

## Material

458 specimens recovered from 11 samples (see Table 1) collected along the strike of the 1.5 m thick limestone lens.

## Discussion

The concept of *P.? nogamii* and its constituent elements has been reviewed extensively in several recent publications (Zhen *et al.* 2003; Zhen and Percival 2004a, b; Cantrill and Burrett 2004). It consists of a seximembrate apparatus including short-based, bi-furrowed Pa and Pb, long-based, bi-furrowed Sa, Sb and Sd, and long-based, uni-furrowed Sc elements; with furrows and coarse striae disappearing just before reaching the basal margin. This species is excluded from *Panderodus* as it lacks a true panderodontid furrow, which cuts deep into basal margin. Typical species of *Panderodus* have only one furrow on the outer lateral face (except for a rare bi-furrowed symmetrical element). Most of the *P.? nogamii* elements have a furrow on each lateral side, and the furrows disappear just before reaching the basal margin (Fig. 11K, Q). Stait and Druce (1993) recognized a uni-furrowed element in the *P.? nogamii* species apparatus. Zhen *et al.* (2003) found this element (referred as the Sc element) was extremely rare in the Early Ordovician material from Mt. Arrowsmith in far western New South Wales. In the Kirkup fauna, *P.? nogamii* is one of the dominant species, but no uni-furrowed element has been identified.

Family ACANTHODONTIDAE Lindström, 1970

Genus *Kirkupodus* Zhen and Pickett gen. nov.

## Derivation of name

After the property name, Kirkup Station, where the type species (and only species assigned to the genus) was recovered.

## Type species

*Kirkupodus tricostatus* Zhen and Pickett gen. et sp. nov.

## Diagnosis

A septimembrate coniform-coniform apparatus

including nongeniculate bicostate M, bicostate Sb and Sc, tricostate Sa and Sd, and drepanodiform Pa and Pb elements; all elements hyaline, with sharp blade-like costae, and ornamented with fine striae; S elements forming a symmetry transitional series; M element with non-expanded base, S and P elements with posteriorly or laterally extended base.

## Discussion

*Kirkupodus* is defined herein as having a septimembrate apparatus. The blade-like costae of the S elements and the general morphology of the P elements resemble the corresponding elements of *Triangulodus* van Wamel, 1974, but *Kirkupodus* lacks a geniculate M element. The P elements and asymmetrical, bicostate Sb and Sc elements of *Kirkupodus tricostatus* can be closely compared with the P and S elements of *Scalpellodus* Dzik, 1976. However, tricostate Sa and Sd elements were not recognised in the species apparatus of the type species, *S. latus*, nor from the apparatuses of the other two species (*S. gracilis* and *S. viruensis*) of *Scalpellodus*, from the Baltic, although descriptions of all these species were based on a large number of specimens (Löfgren 1978). These differences support the establishment of a new genus, *Kirkupodus*, to accommodate the current species from central New South Wales.

As Löfgren (1978, p. 98) pointed out, Dzik's original definition (1976, p. 421) of *Scalpellodus* included elements belonging to both *Scalpellodus* and *Cornuodus*. Löfgren (1978) revised the genus as having a trimembrate apparatus including a scandodiform, a long-based drepanodiform and a short-based drepanodiform elements. She recognised three species from the upper Middle Ordovician (Darriwilian) of Jämtland, northern Sweden, and noted that in the younger species, *S. viruensis* Löfgren, 1978, the long-based drepanodiform element was apparently missing.

The type species, *S. latus*, was originally described as having a trimembrate apparatus including symmetrical short-based, symmetrical long-based, and asymmetrical scandodiform elements (van Wamel 1974), all with prominent surface striation. The holotype (van Wamel 1974, pl. 4, fig. 2a-b) was defined as a symmetrical short-based element, which Löfgren (1978) referred to as the short-based drepanodiform element (= Pb element of our current notation). The symmetrical long-based element (van Wamel 1974, pl. 4, fig. 1a-b) was called the long-based drepanodiform element by Löfgren (1978) (=Pa element of our notation). Only one type of S element was recognized for *S. latus* by both van Wamel (1974) and Löfgren (1978) as the asymmetrical scandodiform



element (= ?Sc element herein).

Sweet (1988) interpreted the genus as consisting of a bimembrate apparatus. More recently, Löfgren (2000, 2003) considered the scandodiform elements to represent the ?S element and the drepanodiform elements to be the ?P elements. Löfgren (2000) illustrated three specimens of *S. latus* from the lower Middle Ordovician (*T. quadrangulum* Subzone) of northern Öland, Sweden, and assigned them to the S element (Löfgren 2000, fig. 4S), M? element (Löfgren 2000, fig. 4T), and P? element (Löfgren 2000, fig. 4U). The doubtful M element of *S. latus* is a nongeniculate element with a short base, and shows some similarity to the M element of *Kirkupodus tricostatus* from central New South Wales (Fig. 12A-C). Later Löfgren (2003) also illustrated three specimens of a slightly younger species, *S. gracilis*, from the upper Middle Ordovician (*L. variabilis* Zone, early Darriwilian) of southern Sweden, as the Sb? element (Löfgren 2003, fig. 7V), the Sd? element (Löfgren 2003, fig. 7X) and the P? element (Löfgren 2003, fig. 7W). Although Löfgren's revised notation for the species apparatus of *Scalpellodus* has not been formally published, it seems clear that Baltic species of *Scalpellodus* do not have tricostate Sa and Sd elements similar to those of *Kirkupodus*.

Stouge (1984) endorsed the definition of *Scalpellodus* given by Löfgren (1978) as consisting of a trimembrate apparatus and recognised a tricostate element in both *Scalpellodus pointensis* Stouge, 1984 and *Scalpellodus biconvexus* (Bradshaw, 1969). It exhibits sharp, edge-like posterior, anterior and outer-lateral costae, and is comparable with the Sd element of *Kirkupodus tricostatus* from central New South Wales. However, neither a symmetrical tricostate Sa element nor a nongeniculate M element was recorded in the apparatus of these two species from Newfoundland. They are considered here as doubtful species of *Kirkupodus*, pending further study.

***Kirkupodus tricostatus* Zhen and Pickett gen. et  
sp. nov.**

Figure 12

**Derivation of name**

Tricostate, referring to the distinctive tricostate Sa (symmetrical) and Sd (asymmetrical) elements of the species.

**Material**

1480 specimens recovered from 14 samples (see Table 1) collected along the strike of the 1.5 m thick limestone lens; including figured holotype

AM F.133090 (Fig. 12D-F), and 18 paratypes, AM F.133088-89, AM F.133091-133106 (Fig. 12A-C, G-AA).

**Diagnosis**

A species of *Kirkupodus* consisting of a septimembrate apparatus including bicostate M, bicostate Sb and Sc, tricostate Sa and Sd, and drepanodiform Pa and Pb elements; M weakly asymmetrical with an antero-posteriorly compressed cusp, Sa symmetrical, Sb asymmetrical with a posteriorly flared base, Sc strongly asymmetrical with base flared more postero-inner laterally, Sd asymmetrical, Pa with a proclined cusp and a unexpanded and inner laterally flared base, and Pb with a sub-erect cusp and a posteriorly-expanded base; all elements ornamented with fine striae.

**Description**

M element weakly asymmetrical; cusp curved posteriorly and slightly outer laterally, antero-posteriorly compressed with a broadly convex anterior face, a less convex posterior face and a sharp blade-like costa on each side forming the lateral edges; base slightly extended posteriorly, clam-shaped in outline in basal view with a broadly arched antero-basal margin (Fig. 12A-C).

Sa element symmetrical and tricostate (Fig. 12G); cusp triangular in cross section (Fig. 12G), proclined with a broad anterior face, a sharp blade-like antero-lateral costa on each side, and a costa along the posterior margin; base posteriorly extended (Fig. 12D-G).

Sb element asymmetrical with a broad anterior face, an antero-laterally located costa on the inner side (Fig. 12L), a postero-laterally located costa on the outer lateral side (Fig. 12J), and a posteriorly extended base, which is oval in outline in basal view (Fig. 12H-I, K).

Sc element strongly asymmetrical with a laterally compressed cusp, and a base which is flared both posterolaterally and on the inner side (Fig. 12M-P), and widest at the posterior end (Fig. 12P); cusp suberect to weakly proclined with sharp costa along its anterior and posterior margins and with smooth lateral faces.

Sd element asymmetrical with a broad anterior face, and with a sharp, blade-like costa on each lateral side and along the posterior margin (Fig. 12Q-T); cusp proclined, triangular in cross section (Fig. 12S), with inner lateral costa more anteriorly located, and varying from weakly asymmetrical (Fig. 12T) to strongly asymmetrical with a twisted cusp (Fig. 12Q); base extended posteriorly, oval to triangular in basal







view (Fig. 12Q, T).

Pa element with a proclined cusp and an inner laterally flared base (Fig. 12X-AA); cusp with sharp anterior and posterior margins, and broadly convex lateral faces, outer lateral face bearing a broad carina located antero-laterally; sharp anterior and posterior edges disappearing before reaching the basal margin; base flared inward, long and posteriorly without prominent expansion (Fig. 12X, AA), flared inward, widest at the mid point (Fig. 12Y-Z) and the outer side of the basal margin more or less straight in basal view (Fig. 12Z).

Pb element similar to Pa, but weakly asymmetrical with a suberect cusp (Fig. 12U-W) and a shorter, less inner laterally flared, but posteriorly, strongly-expanded base (Fig. 12U-V).

### Discussion

*Kirkupodus tricostratus* can be differentiated from the known species of *Scalpellodus* in having a symmetrical tricostrate Sa element and an asymmetrical tricostrate Sd element, and by lacking the long-based elements in the apparatus. In comparison with *S. latus* and other two species from the Middle Ordovician of northern Sweden (Löfgren 1978), the current species has strongly developed blade-like costae in the M and S elements, and finer surface striae, although the P elements are comparable with the Baltic species of *Scalpellodus*.

Order and Family Uncertain

Genus *Pseudooneotodus* Drygant, 1974

### Type species

*Oneotodus? beckmanni* Bischoff and Sannemann, 1958.

### *Pseudooneotodus mitratus* (Moskalenko, 1973)

Figure 9A-B

### Synonymy

*Ambalodus mitratus mitratus* Moskalenko, 1973, p. 86, pl. 17, figs 9-11.

*Pseudooneotodus mitratus* (Moskalenko); Nowlan and McCracken in Nowlan *et al.* 1988, p. 34, pl. 16, figs 2-6 (*cum syn.*); Pohler and Orchard 1990, pl. 6, fig. 12; Trotter and Webby 1995, pl. 4, figs 21-22 (*cum syn.*); Zhen and Webby 1995, p. 285, pl. 4, figs 16-17; Zhen *et al.* 1999, p. 92-94, fig. 9.14-9.15; Zhen *et al.* 2003, fig. 6Q.

### Material

A single specimen from sample C2346.

### Discussion

Occurrence of this species in the Kirkup fauna is very rare, only represented by one element among a huge collection. It is rather common in the Upper Ordovician in central New South Wales, previously reported from the Fossil Hill Limestone (Zhen and Webby 1995), the Ballingool Limestone of the Bowan Park Group (Zhen *et al.* 1999) and from the Late Ordovician allochthonous limestones in the Barnby Hill Shale (Zhen *et al.* 2003). Morphologically, the current specimen is identical with the morphotype showing a smooth surface without nodes on the flanks

Figure 12 (LEFT). *Kirkupodus tricostratus* gen. et sp. nov. A-C, M element; A-B, AM F.133088, paratype, C2343, A, posterior view (IY86017), B, basal view (IY86018); C, AM F.133089, paratype, C2343, upper view (IY86019). D-G, Sa element; D-F, AM F.133090, holotype, C2340, D, lateral view (IY91034), E, basal view (IY91035), F, posterior view (IY91036); G, AM F.133091, paratype, C2347, upper view (IY92001). H-L, Sb element; H, AM F.133092, paratype, C2344, upper view (IY92007); I, AM F.133093, paratype, C2344, basal view (IY91027); J, AM F.133094, paratype, C2343, basal view (IY86020); K, AM F.133095, paratype, C2343, outer lateral view (IY86022); L, AM F.133096, paratype, C2343, inner lateral view (IY86024). M-P, Sc element; M-N, AM F.133097, paratype, C2343, M, inner lateral view (IY86029), N, closing up showing surface striation (IY86030); O-P, AM F.133098, paratype, C2343, O, outer lateral view (IY86027), P, basal view (IY86028). Q-T Sd element; Q, AM F.133099, paratype, C2344, postero-basal view (IY91019); R, AM F.133100, paratype, C2343, inner lateral view (IY86040); S, AM F.133101, paratype, C2343, upper view (IY86033); T, AM F.133102, paratype, C2343, basal-outer lateral view (IY86036). U-W, Pb element; U, AM F.133103, paratype, C2343, inner lateral view (IY86009); V-W, AM F.133104, paratype, C2343, V, outer lateral view (IY86011), W, basal view (IY86014). X-AA, Pa element; X-Y, AM F.133105, paratype, C2343, X, inner lateral view (IY86012), Y, basal view (IY86013); Z-AA, AM F.133106, paratype, C2344, Z, basal view (IY91028), AA, outer lateral view (IY91029). Scale bars 100 µm, unless otherwise indicated.



of the posterior and lateral ridges described from various stratigraphic units of the Late Ordovician in central New South Wales. The occurrence of *P. mitratus* in the Kirkup fauna of early Darriwilian age represents the earliest record of this species.

# ACKNOWLEDGEMENTS

Field work was supported by a grant (Betty Mayne Scientific Research Fund) to ZYY from the Linnean Society of New South Wales. Gary Dargan (Geological Survey of New South Wales) assisted with acid leaching and residue separation. Scanning electron microscope photographs were prepared in the Electron Microscope Unit of the Australian Museum. We are grateful to Dr Marcelo Carrera for supplying photographs of *Zondarella communis*. JWP is an Honorary Research Associate of both the Australian Museum and the Geological Survey of New South Wales, and is grateful to these organisations for the provision of facilities. The authors appreciate the careful commentary of two anonymous reviewers. This is a contribution to IGCP Project 503: Ordovician Palaeogeography and Palaeoclimate.

# REFERENCES

Albanesi, G.L., Hünicken, M.A. and Barnes, C.R. (1998). Biostratigrafía, biofacies y taxonomía de conodontes de las secuencias ordovícicas del Cerro Porterillo, Precordillera central de San Juan, R. Argentina. *Actas de la Academia Nacional de Ciencias* 12, 1–249.

An, T.X. and Ding, L.S. (1985). Ordovician conodont biostratigraphy in Hexian, Anhui Province. *Geological Review* 31 (1), 11–20 (in Chinese).

An, T.X., Zhang, F., Xiang, W.D., Zhang, Y.Q., Xu, W.H., Zhang, H.J., Jiang, D.B., Yang, C.S., Lin, L.D., Cui, Z.T. and Yang, X.C. (1983). ‘The Conodonts of North China and the Adjacent Regions’. 1–223, Science Press, Beijing (in Chinese with English abstract).

An, T.X., and Zheng, S.C. (1990). ‘The conodonts of the marginal areas around the Ordos Basin, northern China’. 1–201, Science Press, Beijing (Chinese with English abstract),

Bassler, R.S. (1927). A new Early Ordovician sponge fauna. *Journal of the Washington Academy of Science* 17, 390–394.

Bischoff, G. and Sannemann, D. (1958). Unterdevonische Conodonten aus dem Frankenwald. *Notizblatt des hessischen Landesamtes für Bodenforschung* 86, 87–110.

Bradshaw, L.E. (1969). Conodonts from the Fort Peña Formation (Middle Ordovician), Marathon Basin, Texas. *Journal of Paleontology* 43, 1137–1168.

Branson, E.R. and Mehl, M.G. (1944). Conodonts. In ‘Index fossils of North America’ (Eds. H.W. Shimer and R.R. Shrock) p. 235–246. (Wiley, New York).

Cantrill, R.C. & Burrett, C.F. (2004). The Greater Gondwana distribution of the Ordovician conodont *Panderodus nogamii* (Lee) 1975. *Courier Forschungsinstitut Senckenberg* 245, 407–419.

Cooper, B.J. (1981). Early Ordovician conodonts from the Horn Valley Siltstone, central Australia. *Palaeontology* 24, 147–183.

Drygant, D.M. (1974). Prostye Konodonty Silura iz nizhego Devona Volyno-Podolya [Simple conodonts from the Silurian and lower Devonian of Volhynia-Podolia]. *Paleontologicheskii Sbornik* 10, 64–69 (in Russian).

Dzik, J. (1976). Remarks on the evolution of Ordovician conodonts. *Acta Palaeontologica Polonica* 21, 395–455.

Dzik, J. (1978). Conodont biostratigraphy and paleogeographical relations of the Ordovician Mójca Limestone (Holy Cross Mts, Poland). *Acta Palaeontologica Polonica* 23, 51–72.

Dzik, J. (1991). Evolution of oral apparatuses in the conodont chordates. *Acta Palaeontologica Polonica* 36, 265–323.

Finks, R.M., Reid, R.E.H., & Rigby, J.K. (2004). ‘Treatise on Invertebrate Paleontology. Part E, Porifera (revised)’, vol. 3 (Demospongiae, Hexactinellida, Heteractinida, Calcarea). 1–872. (Geological Society of America and University of Kansas).

Glen, R.A., Crawford, A.J., Percival, I.G., and Barron, L.M. (2007). Early Ordovician development of the Macquarie Arc, Lachlan Orogen, New South Wales. *Australian Journal of Earth Sciences* 54 (2–3), 167–179.

Hill, D., Playford, G. and Woods, J.T. eds. (1969). ‘Ordovician and Silurian fossils of Queensland’. O.2–O.15, and S.2–S.18. (Queensland Palaeontographical Society, Brisbane).

Igo, H. and Koike, T. (1967). Ordovician and Silurian conodonts from the Langkawi Islands, Malaya, Part I. *Geology and Palaeontology of Southeast Asia* 3, 1–29.

Lee, H.Y. (1975). Conodonten aus dem unteren und mittleren Ordovizium von Nordkorea. *Palaeontographica Abteilung A* 150, 161–186; Stuttgart.

Lehnert, O. (1995). Ordovizische Conodonten aus der Präkordillere Westargentiniens: Ihre Bedeutung für Stratigraphie und Paläogeographie. *Erlanger Geologische Abhandlungen* 125, 1–193.

Lindström, M. (1955). Conodonts from the lowermost Ordovician strata of south-central Sweden. *Geologiska Föreningens i Stockholm Förhandlingar* 76, 517–604.

Lindström, M. (1970). A suprageneric taxonomy of the conodonts. *Lethaia* 3, 427–445.

Lindström, M. (1971). Lower Ordovician conodonts of Europe. In ‘Symposium on conodont



- biostratigraphy' (Eds. W.C. Sweet and S.M. Bergström). *Geological Society of America, Memoir* 127, 21–61.
- Löfgren, A. (1978). Arenigian and Llanvirnian conodonts from Jämtland, northern Sweden. *Fossils and Strata* 13, 1–129.
- Löfgren, A. (1985). Early Ordovician conodont biozonation at Finngrundet, south Bothnian Bay, Sweden (Geology of the southern Bothnian Sea, Part III). *Bulletin of the Geological Institutions of the University of Uppsala* (N.S.) 10, 115–128.
- Löfgren, A. (2000). Early to early Middle Ordovician conodont biostratigraphy of the Gillberga quarry, northern Öland, Sweden. *GFF* 122, 321–338.
- Löfgren, A. (2003). Conodont faunas with *Lenodus variabilis* in the upper Arenigian to lower Llanvirnian of Sweden. *Acta Palaeontologica Polonica* 48 (3), 417–436.
- Moskalenko, T.A. (1973). General survey of Ordovician conodonts of the Siberian Platform: Akademiya Nauk USSR, Siberian Branch, *Trudy Instituta Geologii i Geofiziki* 47, 87–135 (in Russian).
- Moskalenko, T.A. (1989). Konodonty verkhney chasti nizhnego i srednego Ordovika. *Trudy Instituta Geologii i Geofiziki* 751, 125–138.
- Ni, S. and Li, Z. (1987). Conodonts. In Wang X.F., Ni, S.Z., Zeng, Q.L., Xu, G.H., Zhou, T.M., Li, Z.H., Xiang, L.W. and Lai, C.G., 'Biostratigraphy of the Yangtze Gorge area 2: Early Palaeozoic Era'. 386–447, 549–555, 619–632. (Geological Publishing House, Beijing) (in Chinese with English abstract).
- Nicoll, R.S. and Kelman, A. (2004). Arrangement of elements in the Early Ordovician Likmas type ramiform-ramiform conodont *Erraticodon patu* Cooper, 1981: interpretation and implications. *Memoirs of the Association of Australasian Palaeontologists* 30, 207–220.
- Nowlan, G.S., McCracken, A.D. and Chatterton, B.D.E. (1988). Conodonts from Ordovician-Silurian boundary strata, Whittaker Formation, MacKenzie Mountains, Northwest Territories. *Geological Survey of Canada, Bulletin* 373, 1–99.
- Pohler, S.M.L., and Orchard, M.J. (1990). Ordovician conodont biostratigraphy, western Canadian Cordillera. *Geological Survey of Canada Paper* 90 – 15, 1–37.
- Pickett, J.W., & Percival, I.G. (2001). Ordovician faunas and biostratigraphy in the Gunningbland area, central New South Wales, Australia. *Alcheringa* 25, 9–52.
- Rigby, J.K., & Webby, B.D. (1988). Late Ordovician sponges from the Malongulli Formation of central New South Wales, Australia. *Palaeontographica Americana* 56, 1–147.
- Sergeeva, S.P. (1974). Nekotorye novye konodonty iz ordovikskikh otlozhenii leningradskoy oblasti [Some new Ordovician conodonts from the Leningrad region]. *Paleontologicheskii Sbornik* 11 (2), 79–84.
- Serpagli, E. (1974). Lower Ordovician conodonts from Precordilleran Argentina (Province of San Juan). *Bollettino della Società Paleontologica Italiana* 13, 17–98.
- Simpson, C.J., Cas, R.A.F., & Arundell, M.C. (2005). Volcanic evolution of a long-lived Ordovician island-arc province in the Parkes region of the Lachlan Fold Belt, southeastern Australia. *Australian Journal of Earth Sciences* 52, 863–886.
- Smith, R.E. (1966). The geology of Mandurama-Panuara. *Journal and Proceedings of the Royal Society of New South Wales* 98, 239–262.
- Stait, K. and Druce, E.C. (1993). Conodonts from the Lower Ordovician Coolibah Formation, Georgina Basin, central Australia. *BMR Journal of Australian Geology and Geophysics* 13, 293–322.
- Stearn, C.W., & Pickett, J.W., 1994. The stromatoporoid animal revisited: building the skeleton. *Lethaia* 27, 1–10.
- Stearn, C.W., Webby, B.D., Nestor, H., and Stock, C.W. (1999). Revised classification and terminology of Palaeozoic stromatoporoids. *Acta Palaeontologica Polonica* 44 (1), 1–70.
- Stouge, S. (1984). Conodonts of the Middle Ordovician Table Head Formation, western Newfoundland. *Fossils and Strata* 16, 1–145.
- Sweet, W.C. (1988). 'The Conodonta: Morphology, Taxonomy, Paleoecology, and Evolutionary History of a Long-Extinct Animal Phylum'. 212pp. (Clarendon Press, Oxford).
- Trotter, J.A., and Webby, B.D. (1995). Upper Ordovician conodonts from the Malongulli Formation, Cliefden Caves area, central New South Wales. *AGSO Journal of Geology and Geophysics* 15 (4), 475–499.
- van Wamel, W.A. (1974). Conodont biostratigraphy of the Upper Cambrian and Lower Ordovician of north-western Öland, south-eastern Sweden. *Utrecht Micropalaeontological Bulletins* 10, 1–125.
- Viira, V. (1974). 'Konodonty Ordovika Pribaltiki [Ordovician conodonts of the east Baltic]'. 142pp. (Valgus, Tallinn).
- Wang, C.Y., ed. (1993). 'Conodonts of the Lower Yangtze Valley - an index to biostratigraphy and organic metamorphic maturity'. 326pp. (Science Press, Beijing) (in Chinese with English summary).
- Watson, S.T. (1988). Ordovician conodonts from the Canning Basin (Western Australia) *Palaeontographica, Abteilung A*, 203 (4–6), 91–147.
- Webby, B.D., 1993. Evolutionary history of Palaeozoic Labechiida (Stromatoporoidea). *Memoir of the Association of Australasian Palaeontologists* 15, 57–67.
- Zhang, J.H. (1998a). Conodonts from the Guniutan Formation (Llanvirnian) in Hubei and Hunan provinces, south-central China. *Stockholm Contributions in Geology* 46, 1–161.
- Zhang, J.H. (1998b). The Ordovician conodont genus *Pygodus*. In 'Proceedings of the Sixth European Conodont Symposium (ECOS VI)'. (Ed. H. Szaniawski). *Palaeontologia Polonica* 58, 87–105.



- Zhao, Z.X., Huang, Z.B., Du, P.D., Zhang, G.Z., Xiao, J.N. and Tan, Z.J. (2005). New species of the Lower-Middle Ordovician conodonts from the Tarim Basin in Xinjiang. *Acta Micropalaeontologica Sinica* 22, 29–38. (in Chinese with English abstract)
- Zhen, Y.Y. and Percival, I.G. (2004a). Middle Ordovician (Darriwilian) conodonts from allochthonous limestones in the Oakdale Formation of central New South Wales, Australia. *Alcheringa* 28, 77–111.
- Zhen, Y. Y. and Percival, I. G. (2004b). Middle Ordovician (Darriwilian) conodonts from the Weemalla Formation, south of Orange, New South Wales. *Memoirs of the Association of Australasian Palaeontologists* 30, 153-178.
- Zhen, Y.Y. and Percival, I.G. (2006). Late Cambrian-Early Ordovician conodont faunas from the Koonenberry Belt of western New South Wales. *Memoir of the Association of Australasian Palaeontologists* 32, 267–285.
- Zhen, Y.Y. and Webby, B.D. (1995). Upper Ordovician conodonts from the Cliefden Caves Limestone Group, central New South Wales, Australia. *Courier Forschungsinstitut Senckenberg* 182, 265–305.
- Zhen, Y.Y., Liu, J.B. and Percival, I.G. (2007). Revision of conodont species *Erraticodon hexianensis* from the upper part of the Meitan Formation (Middle Ordovician) of Guizhou, South China. *Palaeontological Research* 11 (2), 143–160.
- Zhen, Y.Y., Percival, I.G. and Webby, B.D. (2003). Early Ordovician conodonts from far western New South Wales, Australia. *Records of the Australian Museum* 55, 169–220.
- Zhen, Y.Y., Webby, B.D. and Barnes, C.R. (1999). Upper Ordovician conodonts from the Bowan Park succession, central New South Wales, Australia. *Géobios* 32 (1), 73–104.